

Supporting Information

Pretargeted PET Imaging of *trans*-Cyclooctene-Modified Porous Silicon Nanoparticles

Outi Keinänen,¹ Ermei M. Mäkilä,² Rici Lindgren,² Helena Virtanen,³ Heidi Liljenbäck,^{3,4} Vesa Oikonen,³ Mirkka Sarparanta,^{1,5} Carla Molthoff,⁶ Albert D. Windhorst,⁶ Anne Roivainen,^{3,4} Jarno J. Salonen,² Anu J. Airaksinen^{1*}

¹*Department of Chemistry - Radiochemistry, University of Helsinki, A.I. Virtasen aukio 1, 00560 Helsinki, Finland*

²*Department of Physics and Astronomy, University of Turku, Vesilinnantie 5, 20014 Turun yliopisto, Finland*

³*Turku PET Centre, University of Turku, Kiinamylynkatu 4-8, 20520 Turku, Finland*

⁴*Turku Center for Disease Modeling, University of Turku, Kiinamylynkatu 10, 20520, Turku, Finland*

⁵*Department of Radiology, Memorial Sloan Kettering Cancer Center, 417 E 68th Street, 10065 New York, New York, United States*

⁶*Department of Radiology and Nuclear Medicine, VU University Medical Center, De Boelelaan 1117, Amsterdam 1081 HV, The Netherlands*

Experimental procedures

Materials

Unless otherwise noted, all reagents were purchased from commercial suppliers and used without further purification. All water used was ultrapure ($> 18.2 \text{ M}\Omega \text{ cm}^{-1}$). Compound **1** and its precursors were prepared according to previously described procedures.¹ [^{18}F]**1** was synthesized with $51.6 \pm 5.4\%$ decay-corrected yield ($n=6$, 1.1–2.9 GBq at the end of synthesis). The total duration of the synthesis was 2 hours. Radiochemical purity was $>99\%$ and the specific activity varied between 12–809 GBq/ μmol at EOS.

Preparation of TCO-nanoparticles

The porous silicon nanoparticles were prepared by electrochemically anodizing p+ type Si(100) wafers of 0.01–0.02 Ωcm resistivity in a 1:1 (vol.) hydrofluoric acid (38%) – ethanol electrolyte. A pulsed etching profile was used to produce PSi multilayer films with alternating low and high porosity regions to facilitate the production of the nanoparticles. The multilayer films were thermally hydrocarbonized with acetylene as described earlier.² The treated films were then immersed into undecylenic acid for 16 h at 120 °C for partial COOH termination. The films were ball milled in 10 vol-% undecylenic acid-decane solution into nanoparticles. The final size selection was done using centrifugation.

The –COOH terminated PSi NPs (UnTHCPSi) were functionalized by activating the carboxylic acid groups with EDC/NHS cross-linking chemistry (1-Ethyl-3-(3-dimethylaminopropyl)carbodiimide/N-hydroxysuccinimide) by dispersing the NPs in 5 mM EDC/NHS-ethanol solution for 1 h. The activated NPs were then dispersed into 100 mM 3-azidopropylamine–chloroform solution to generate an azide terminated surface.

The N₃-PSi NPs were then dispersed into 3.33 mM *trans*-cyclooctene-PEG₁₂-dibenzocyclooctyne (TCO-PEG₁₂-DBCO)–chloroform solution for a strain-promoted azide-alkyne cycloaddition for 4 h. The excess reagents were washed from the particles using chloroform and ethanol.

Characterization of TCO-nanoparticles

Structural characteristics of the PSi NPs were determined with nitrogen sorption at -196 °C using a Micromeritics TriStar 3000. The specific surface area of the NPs was calculated using the Brunauer–Emmett–Teller theory and the total pore volume by taking the total adsorbed amount of N₂ at relative pressure $p/p_0 = 0.97$. The average pore diameter was calculated as $d=4V/A$ assuming

the pore shape as cylindrical. The obtained surface area of the NPs was $242 \pm 4 \text{ m}^2/\text{g}$ and the total pore volume $0.71 \pm 0.01 \text{ cm}^3/\text{g}$. The calculated average pore diameter was $11.8 \pm 0.4 \text{ nm}$.

The hydrodynamic diameter (Z-average) and the particle zeta potential were determined with dynamic and electrophoretic light scattering, respectively, using Malvern Zetasizer Nano ZS. The Z-average and the polydispersity index (PdI) of the particles at different stages of modification are listed in Table S1.

TABLE S1. Hydrodynamic diameter and polydispersity index of the PSi NPs.

	Z-average (nm)	PdI	Zeta potential (mV)
UnTHCPSi	158 ± 3	0.13 ± 0.02	-40.5 ± 2.5
N₃-THCPSi	163 ± 1	0.10 ± 0.01	-40.1 ± 4.7
TCO-THCPSi	167 ± 3	0.13 ± 0.02	-39.8 ± 5.7
TCO-THCPSi (Ag-treated)	165 ± 2	0.15 ± 0.02	-40.0 ± 5.1

Surface chemistry modifications were analyzed with Fourier transform infrared spectroscopy (FTIR) using a Mattson Galaxy 6020 spectrometer equipped with Gasera PA301 photoacoustic detector. Helium was utilized as the sample chamber gas, while the spectra was measured with a resolution of 4 cm^{-1} , averaging 128 scans. Full and zoomed spectra of the PSi NPs at different modification stages are shown in Figure S1. Initially, the $-\text{COOH}$ terminated particles show a broad band centered around 1715 cm^{-1} , related to the carbonyl stretch vibration of the carboxylic acid group. After activation, a triplet of peaks is observable at slightly higher wavenumbers at 1745, 1790, and 1820 cm^{-1} , that can be ascribed to the formation of succinimidyl terminated groups. Conjugating the azidopropylamine to the NPs causes the triplet peaks to disappear, while broad bands around 1650 and 1545 cm^{-1} are formed, confirming its amide bonding. Also, a strong peak is visible at 2100 cm^{-1} due to the azide stretching vibrations.

Elemental analysis was performed to determine the amount of conjugated TCO. The calculation was based on the increase of nitrogen between azide step and final product. The following formula was used:

$$\frac{\%N(\text{N}_3 \text{ NP}) - \%N(\text{TCO NP})}{3 \cdot M(\text{N})}$$

where $\%N(\text{N}_3 \text{ NP})$ =percentage amount of nitrogen in azide modified nanoparticle sample, $\%N(\text{TCO NP})$ =percentage amount of nitrogen in TCO-modified nanoparticle sample, $M(\text{N})$ =molar

mass of nitrogen, and number 3 is used because TCO-PEG12-DBCO moiety has three nitrogen atoms.

The elemental analysis results were 0.64% and 0.67% of nitrogen for azide step and final product, respectively. Using the above formula results 0.0071 mmol/g. Each animal in the group that received nanoparticles received a dose of 0.2 mg of TCO-NPs (1.42 nmol of TCO).

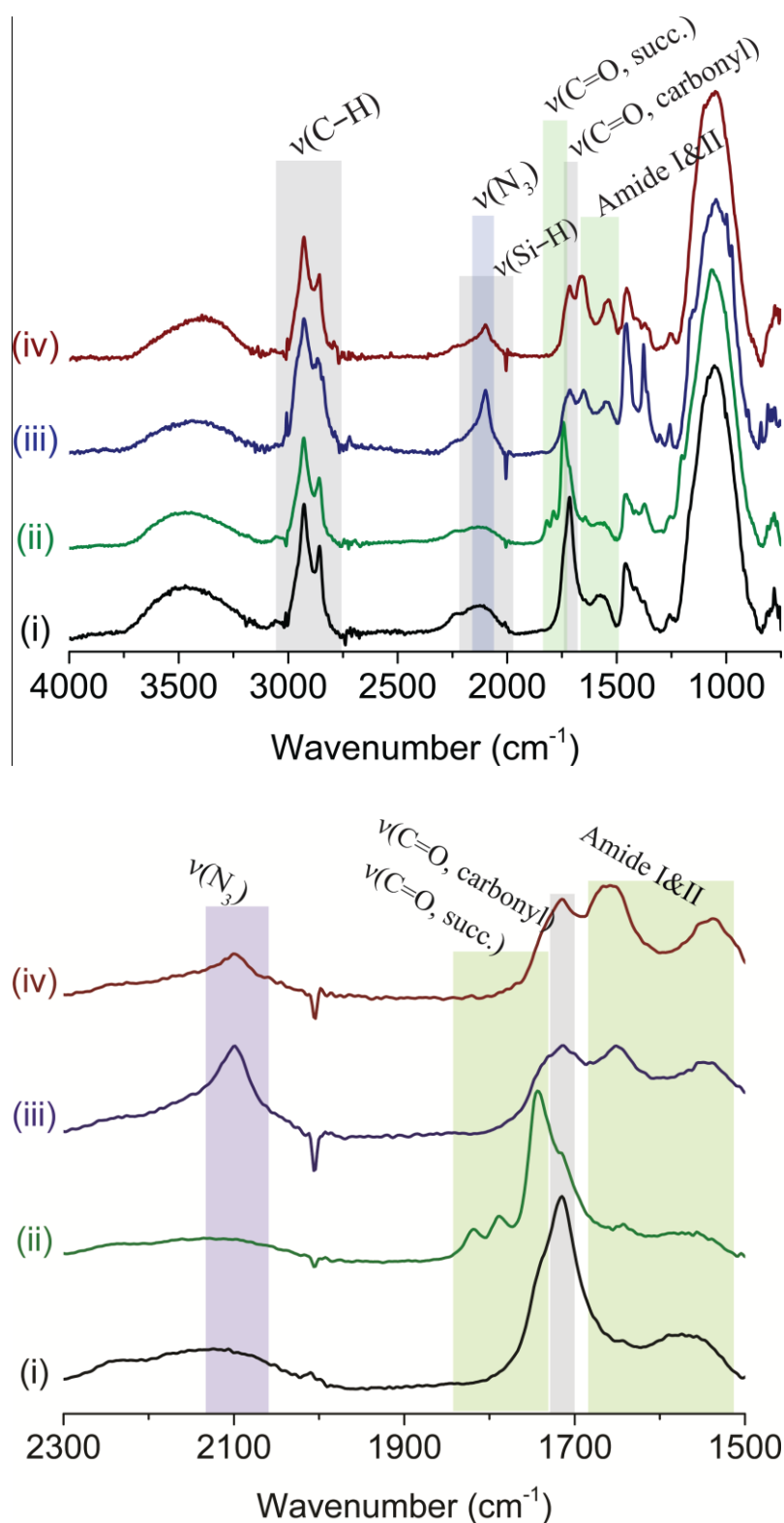


FIGURE S1. Photoacoustic FTIR spectra of the PSi NPs at different stages of the surface modification. (i) UnTHCPSi, (ii) succinimidyl-terminated THCPSi, (iii) N_3 -terminated THCPSi and (iv) TCO-PEG₁₂-DBCO modified THCPSi.

In vitro reactivity of TCO-NPs

TCO-NPs (0.001-0.2 mg/ml) were incubated with [^{18}F]**1** of two different specific activities (18.4 GBq/ μmol and 0.18 GBq/ μmol) in PBS pH 7.41 (total volume in each experiment was 1 ml). To confirm that AgNO_3 modification did not decrease the reactivity of the Ag-treated TCO-NPs (0.0007-0.013 mg/ml) were tested with a specific activity of 19.2 GBq/ μmol . The reaction was let to proceed for 5 minutes at room temperature after which the samples were centrifuged (10 000 g, 5 min) and radioactivity of the supernatant (unreacted [^{18}F]**1**) and the pellet (reacted [^{18}F]**1** with the NPs) were measured in order to determine the yield of the IEDDA reaction. Control measurement was performed with unmodified nanoparticles (UnTHCPSi) and [^{18}F]**1**. 0.4% of radioactivity was left on unmodified nanoparticle pellet.

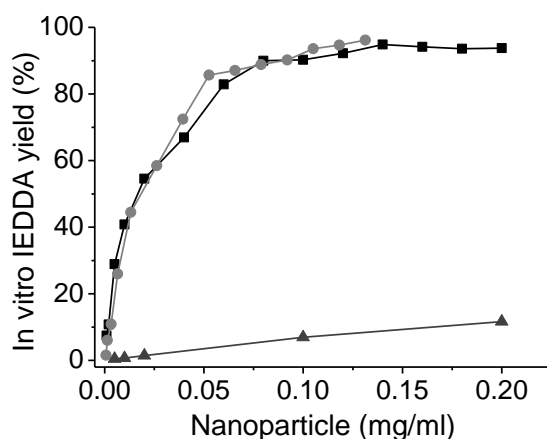


FIGURE S2. In vitro IEDDA yield of the NPs with [^{18}F]**1** in PBS pH 7.41 (7.1 nmol TCO / mg NPs, total volume: 1 ml, reaction time: 5 min). Black square: TCO-NP with [^{18}F]**1** (18.4 GBq/ μmol), light gray circle: Ag-treated TCO-NP with [^{18}F]**1** (19.2 GBq/ μmol), and dark gray triangle: TCO-NP with [^{18}F]**1** (0.18 GBq/ μmol).

Animal experiments

All animal experiments were performed according to the respective national and European legislation with an approved ethical license from the National Board on Animal Experimentation (Regional State Administrative Agency of Southern Finland, Finland and VUmc, Amsterdam, The Netherlands). Biodistribution of [^{18}F]**1** was investigated in male 12-week old BALB/c mice (strain OlaHsd, Harlan, The Netherlands) after intravenous (i.v.) administration. The mice were group-housed in standard polycarbonate cages with aspen bedding with tap water and rodent feed (Harlan Teklad Global Diet 2018) available ad libitum. Lighting was set to a 12:12 rhythm and the temperature and humidity were controlled at a range of 22 ± 1 °C and $55\pm 10\%$, respectively. For the

intravenous injection, the animal was anesthetized with inhalation of isoflurane (IsoFlo Vet., Orion Pharma, Espoo, Finland) at 4% in 60:40 medical air:oxygen carrier at a flow rate of 1 l/min. Anesthesia was maintained with inhalation of 3% of isoflurane in 60:40 medical air-oxygen at a flow rate of 1 l/min. The lateral tail vein was cannulated and the cannula was flushed with 50 µl of 50 IU/ml heparin (Leo Pharma). The in vitro labelled [^{18}F]1-TCO-nanoparticles were administered at a dose of 5.0 ± 3 MBq in 50 µl 5.4% glucose solution followed by a flush of the catheter with 50 µl of 5.4% glucose solution. TCO-nanoparticles were administered at a dose of 0.2 mg in 50 µl 5.4% glucose solution followed by a flush of the catheter with 50 µl of 5.4% glucose solution. [^{18}F]1 was administered at a dose of 6.2 ± 2.5 MBq in 50-100 µl 10% EtOH 0.9 % NaCl followed by a flush of the catheter with 50 µl of 0.9% NaCl. The animals were sacrificed under anesthesia by cervical dislocation at designated time points after tracer administration and samples of tissues and body fluids were collected for radioactivity measurements. Tissue samples were counted on an automated gamma counter (Wizard 3, PerkinElmer, Turku, Finland) for 60 s with three repeats for each sample.

For PET imaging studies with TCO-NPs, isoflurane/oxygen inhalation anesthetics (0.5 l/min O₂, 2% isoflurane) was applied. Prior to imaging the jugular vein of the mouse was cannulated for i.v. administration of the tracer. The mouse was positioned in the Mediso nanoScan® PET-CT (Mediso, Budapest, Hungary) and prior to injection of the tracer, a routine CT Helican scan was made. Thereafter, the tracer (5.2 ± 0.6 MBq, specific activity 302-809 GBq/µmol at EOS) was injected and PET acquisition was performed for 60 min (Mediso Nucline acquisition software). Reconstruction software provided by Mediso (3D Tera-Tomo reconstruction method using OSEM) was applied according to the manufacturer's instructions, including corrections for decay, randoms, dead time, and attenuation. The bed was manually removed from the PET-CT image.

For 120 min dynamic PET imaging the device was Inveon Multimodality PET/CT (Siemens Medical Solutions, Knoxville, TN, USA). Mice were anesthetized with isoflurane, two tail veins were cannulated and CT was performed for anatomical reference and attenuation correction. A 120 min dynamic PET started at the time of [^{18}F]1 injection. The PET data acquired in a list-mode was reconstructed iteratively with ordered-subsets expectation maximization 3D algorithm followed by maximum a posteriori reconstruction (OSEM3D/MAP) into 6×10 s, 4×60 s, 5×300 s, 9×600 s time frames. Based on CT as the anatomical reference, a quantitative PET analysis was performed by defining regions of interest (ROIs) with Inveon Research Workplace 4.1 software (Siemens Medical Solutions, Malvern, PA, USA). The radioactivity concentration was expressed as a standardized uptake value (SUV) calculated using the average radioactivity concentration of the

ROI normalized with the injected radioactivity dose and animal weight, and as time-activity curve (TAC). After PET/CT imaging, mice were sacrificed, various tissues were excised, weighed and measured for radioactivity by using a gamma counter (3" NaI, Triathler 425-010, Hidex, Turku, Finland). The radioactivity measurements were corrected for the radionuclide decay to the time of injection, ex vivo biodistribution results were expressed as percentage of injected radioactivity dose per gram of tissue (%ID/g).

TABLE S2. Injected amount (nmol), specific activity (SA, at the time of injection), and injected radioactivity (MBq, at the time of injection) of [^{18}F]1 in pretargeted experiments with AgNO_3 treated NPs.

Experiment	Time between NP and [^{18}F]1	Injected amount of NP (mg)	Injected [^{18}F]1 (nmol)	SA of [^{18}F]1 (GBq/ μmol)	Injected dose (MBq)
TCO-NP + [^{18}F]1	15 min	0.2	0.17-0.19	22.2-40.2	5.9 ± 0.5
TCO-NP + [^{18}F]1	24 h	0.2	0.13-0.27	17.7-55.4	6.5 ± 1.8

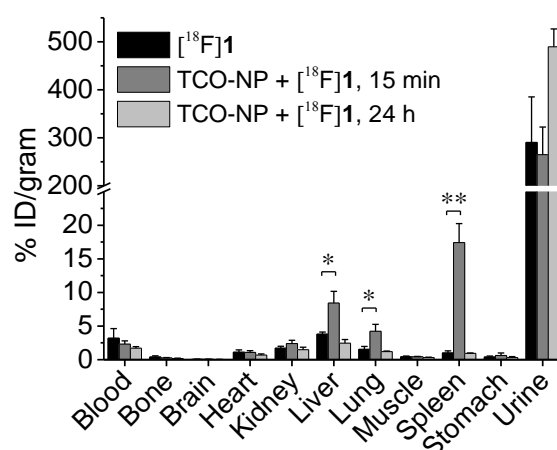


FIGURE S3. The biodistribution of radioactivity 60 min after i.v. injection of [^{18}F]1 (black), and pretargeted TCO-NPs (Ag treated): NPs injected 15 min prior [^{18}F]1 (dark gray) and 24 hours prior [^{18}F]1 (light gray). Values represent mean \pm s.d. (n=3). *p < 0.05 **p < 0.001

Ex vivo biodistribution

TABLE S3. The biodistribution of radioactivity after i.v. injection of [^{18}F]**1** and pretargeted NPs at four time points. Values represent mean \pm s.d. (n=3, except for 120 min n=2).

	15 min		30 min		60 min			120 min	
Organ	[^{18}F] 1 %ID/g	NP + [^{18}F] 1 %ID/g	[^{18}F] 1 %ID/g	NP + [^{18}F] 1 %ID/g	[^{18}F] 1 %ID/g	NP + [^{18}F] 1 %ID/g	Ag-NP + [^{18}F] 1 %ID/g	[^{18}F] 1 %ID/g	NP + [^{18}F] 1 %ID/g
Blood	5.9 \pm 0.9	6.6 \pm 0.7	4.2 \pm 1.1	5.1 \pm 0.4	3.2 \pm 1.4	2.7 \pm 0.3	2.3 \pm 0.5	0.57 \pm 0.02	0.79 \pm 0.07
Bone	0.7 \pm 0.2	0.6 \pm 0.3	0.2 \pm 0.2	0.5 \pm 0.2	0.4 \pm 0.2	0.15 \pm 0.07	0.25 \pm 0.05	0.17 \pm 0.06	0.20 \pm 0.07
Brain	0.13 \pm 0.03	0.13 \pm 0.01	0.07 \pm 0.02	0.10 \pm 0.02	0.06 \pm 0.01	0.08 \pm 0.01	0.06 \pm 0.01	0.034 \pm 0.001	0.043 \pm 0.010
Heart	2.9 \pm 0.4	3.7 \pm 0.1	1.7 \pm 0.2	2.6 \pm 0.5	1.1 \pm 0.3	1.2 \pm 0.2	1.1 \pm 0.3	0.52 \pm 0.10	0.42 \pm 0.01
Kidney	7.0 \pm 0.9	9.8 \pm 2.8	4.1 \pm 0.8	5.6 \pm 0.9	1.7 \pm 0.3	2.4 \pm 0.2	2.4 \pm 0.5	0.53 \pm 0.12	0.43 \pm 0.06
Large intestines	2.2 \pm 0.3	2.2 \pm 0.2	1.9 \pm 0.9	2.0 \pm 0.6	16.1 \pm 12.4	3.5 \pm 1.0	1.9 \pm 0.5	0.49 \pm 0.20	0.51 \pm 0.11
Liver	22.0 \pm 3.3	22.1 \pm 6.2	9.2 \pm 2.0	15.8 \pm 4.6	3.8 \pm 0.3	7.6 \pm 2.2	8.4 \pm 1.7	0.67 \pm 0.08	1.9 \pm 0.2
Lung	5.1 \pm 0.6	23.5 \pm 9.7	2.6 \pm 0.9	13.9 \pm 5.3	1.5 \pm 0.4	4.6 \pm 1.5	4.2 \pm 1.0	0.75 \pm 0.07	1.8 \pm 0.4
Muscle	0.71 \pm 0.02	0.9 \pm 0.2	0.5 \pm 0.1	0.6 \pm 0.2	0.4 \pm 0.1	0.7 \pm 0.3	0.4 \pm 0.1	0.43 \pm 0.02	0.54 \pm 0.08
Small intestines	11.1 \pm 4.8	8.5 \pm 2.2	4.3 \pm 1.1	5.1 \pm 1.3	8.1 \pm 1.0	3.5 \pm 0.5	2.1 \pm 0.7	3.1 \pm 2.4	3.4 \pm 2.7
Spleen	2.8 \pm 0.5	11.0 \pm 1.9	1.9 \pm 0.4	10.4 \pm 2.3	1.0 \pm 0.3	9.8 \pm 0.7	17.4 \pm 2.8	0.49 \pm 0.08	15 \pm 1.6
Stomach	1.8 \pm 1.0	2.1 \pm 1.1	0.8 \pm 0.1	1.4 \pm 0.5	0.4 \pm 0.15	0.5 \pm 0.03	0.6 \pm 0.4	0.24 \pm 0.05	0.24 \pm 0.01
Urine	189.1 \pm 104.1	98.7 \pm 39.0	232.6 \pm 217.3	191.8 \pm 77.9	290.5 \pm 94.7	255.2 \pm 164.3	264.7 \pm 57.8	360 \pm 120	330 \pm 47

Preclicking of TCO-nanoparticles

TCO-nanoparticles were radiolabeled with [^{18}F]**1** by mixing them with [^{18}F]**1** in 10% ethanol solution. The mixture was incubated for 5 minutes in 37 °C. After incubation the mixture was centrifuged (10 000 g, 5 min) and the pellet and supernatant were measured with dose calibrator. The particles were dissolved in 5.4% glucose solution, and again centrifuged (10 000 g, 5 min) and the pellet and supernatant were measured with dose calibrator. The particles were dissolved in 5.4% glucose solution by using Vortex and injected to animals. Based on these results the concentration of TCO-NPs in spleen in pretargeted experiments were evaluated. The %ID/g values were used to calculate how many milligrams of TCO-NPs (total injected amount was 0.2 mg) should be found from the spleen.

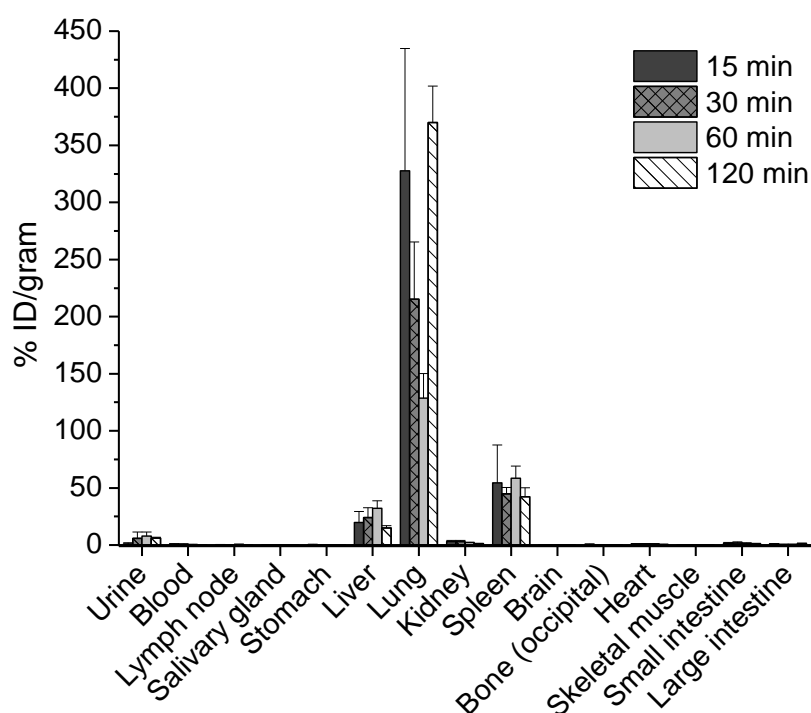


FIGURE S4. The biodistribution of the in vitro ^{18}F -labeled nanoparticles in BALB/c male mice at four time points (n=3) after i.v. administration of 5.0 ± 3.0 MBq. Values represent mean \pm s.d. (n=3). The high lung accumulation indicates poor colloidal stability and the possible formation of aggregates in the formulation.

PET images

Pretargeted PET of TCO-NPs revealed high accumulation of the particles in lungs (Fig. S5) compared to Ag-TCO-NP (Fig. S6). The high lung accumulation indicates poor colloidal stability and the possible formation of aggregates in the formulation, which was used during the first PET study.

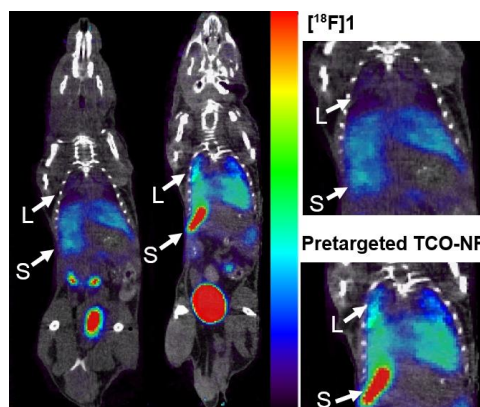


FIGURE S5. Representative summed (35-55 min) PET-CT image of TCO-NPs and a control, and zoomed in image of lung-liver-spleen area. Left and right up: Control, only $[^{18}\text{F}]\mathbf{1}$. Middle and right down: TCO-NPs administered 15 min before the injection of $[^{18}\text{F}]\mathbf{1}$. L=lung, S=spleen. These NPs were not treated with AgNO_3 resulting in higher lung accumulation.

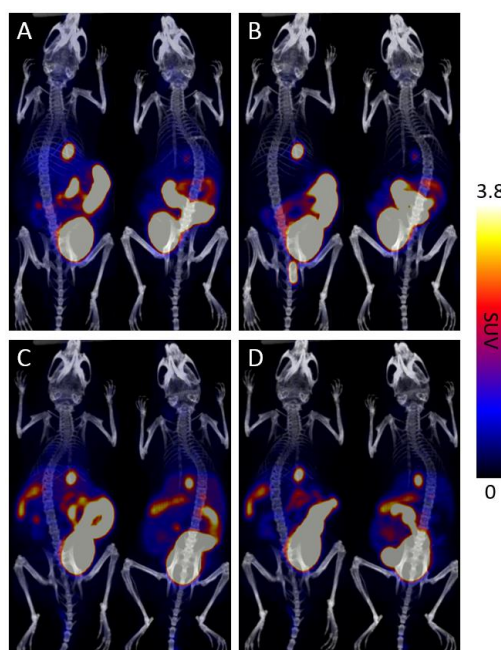


FIGURE S6. Summed whole body PET-CT images of TCO-nanoparticles ($n = 2$) and the controls ($n = 2$). (A) Control, only $[^{18}\text{F}]\mathbf{1}$ (summed 50-60 min). (B) Control, only $[^{18}\text{F}]\mathbf{1}$ (summed 110-120 min). (C) Pretargeted TCO-nanoparticles administered 15 min before the injection of $[^{18}\text{F}]\mathbf{1}$

(summed 50-60 min). (D) Pretargeted TCO-nanoparticles administered 15 min before the injection of [^{18}F]**1** (summed 110-120 min).

Kinetic modeling

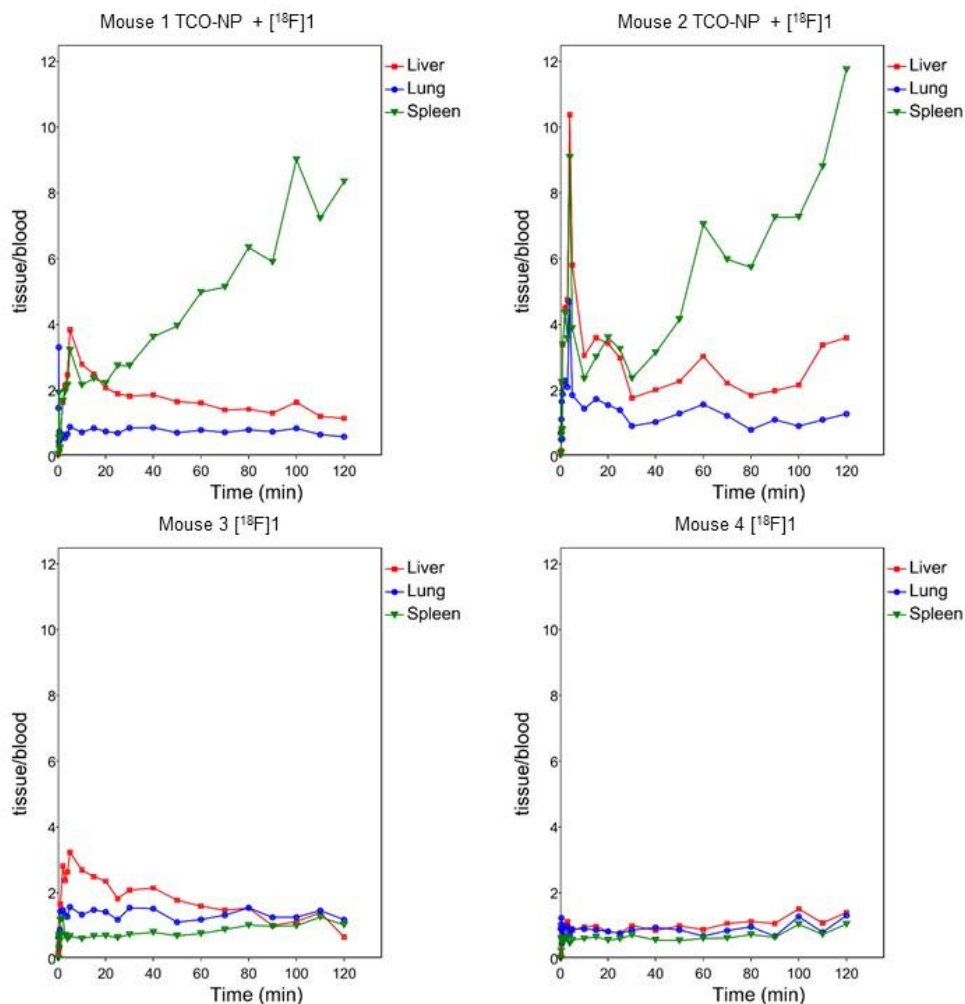


FIGURE S7. Tissue to blood curves.

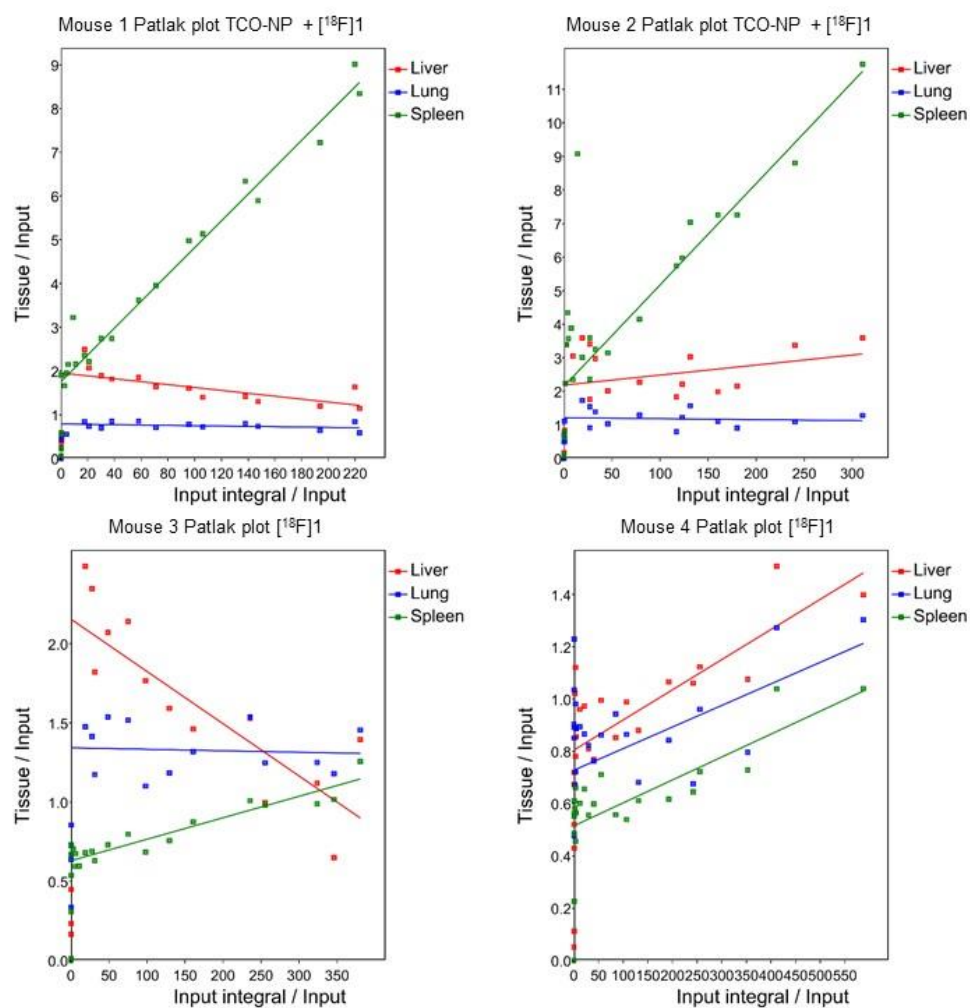


FIGURE S8. Patlak plots.

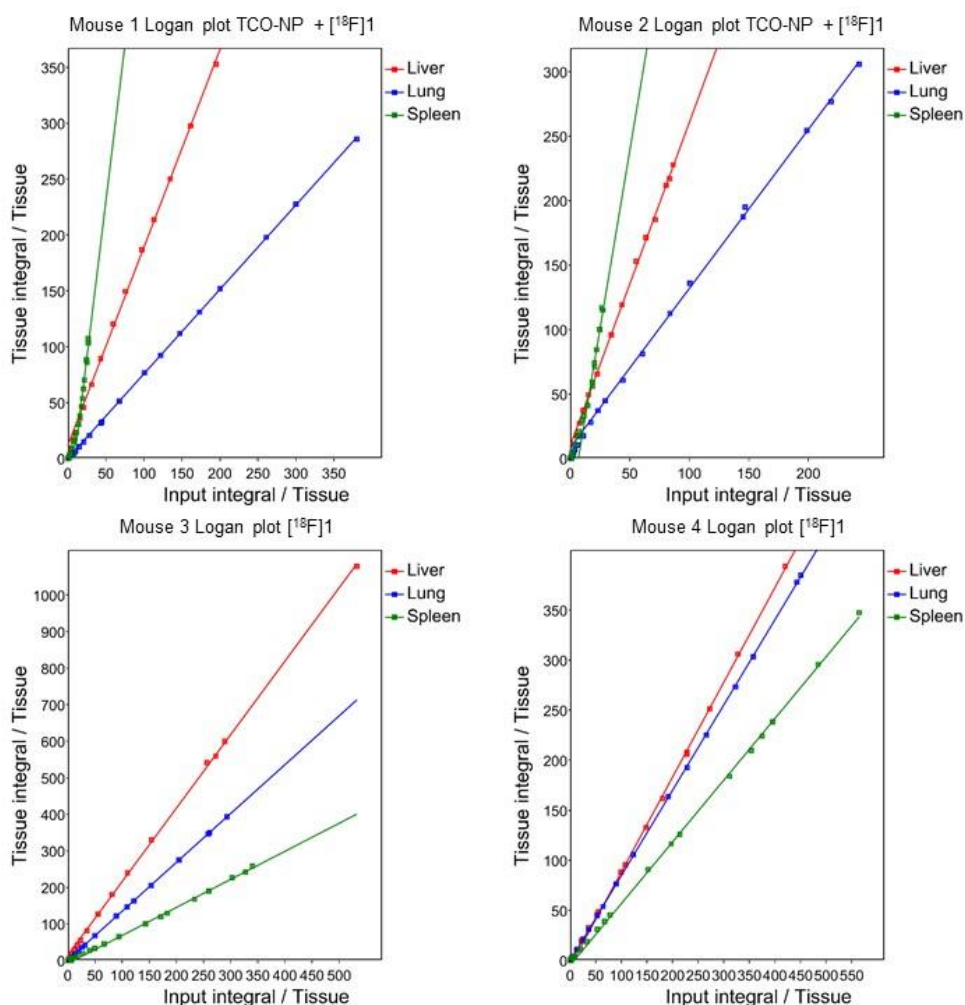


FIGURE S9. Logan plots.

References:

- (1) Keinänen, O.; Li, X. G.; Chenna, N. K.; Lumen, D.; Ott, J.; Molthoff, C. F.; Sarparanta, M.; Helariutta, K.; Vuorinen, T.; Windhorst, A. D.; Airaksinen, A. J., A New Highly Reactive and Low Lipophilicity Fluorine-18 Labeled Tetrazine Derivative for Pretargeted PET Imaging. *ACS Med Chem Lett* **2016**, 7, 62-66.
- (2) Bimbo, L. M.; Sarparanta, M.; Santos, H. A.; Airaksinen, A. J.; Mäkilä, E.; Laaksonen, T.; Peltonen, L.; Lehto, V.-P.; Hirvonen, J.; Salonen, J., Biocompatibility of Thermally Hydrocarbonized Porous Silicon Nanoparticles and their Biodistribution in Rats. *ACS Nano* **2010**, 4, 3023-3032.